AUT Journal of Mechanical Engineering

AUT J. Mech. Eng., 8(2) (2024) 151-180
DOI: 10.22060/ajme.2024.23065.6096

Experimental investigation of fin heat transfer characteristics in different condition

Mohammad Pourjafargholi *, Alireza Gholami, Mohammadreza Karimi

Department of Mechanical Engineering, Khatam al-Anbia Air Defense University, Tehran, Iran

ABSTRACT: Applying heat sinks as extended surfaces plays a significant role in cooling various industrial equipment. This study investigates the impact of heat transfer parameters of fins, such as practical geometry, wall heat flux, coolant velocity, and the angle at which the coolant flow interacts with the fin. The geometry of the fins includes rectangular and triangular shapes, with a heat flux range of approximately 4.6-18.5 kW/m2, coolant velocities ranging from 1-2 m/s, and angles of 0º, 45º, and 90º between the fin position and cooling flow direction. Aluminum, known for its high conductivity, was chosen as the material for the fin structure, with air serving as the primary cooling flow. The study found that triangular fins exhibited a higher convective heat transfer rate than rectangular fins, approximately 47.4% higher on average across all conditions. However, rectangular fins dissipated heat from the wall more effectively. Pressure drop was assessed by comparing cooling flow velocities associated with each fin in various positions. Results revealed that the sharp tip of triangular fins reduced the vorticity effect, increased average flow velocity, and decreased pressure drop. Additionally, rectangular fins were approximately 10.4% more efficient on average than triangular fins. The study also concluded that the impact angle had a negligible effect on the efficiency of both rectangular and triangular fins.

Review History:

Received: Mar. 18, 2024
Revised: May, 31 2024
Accepted: Jul. 21, 2024
Available Online: Jul. 25, 2024

Keywords:

Fin
Heat Transfer Coefficient
Pressure Drop
Temperature Distribution

1- Introduction

Engines play a primary role in various industrial systems by converting heating energy into mechanical energy. In other words, the explosion in the internal combustion engine generates additional high-heating energy. Therefore, the performance, practicality, health, and safety of the internal combustion engine rely heavily on the heat dissipation rate provided by the cooling system. Cooling systems are categorized based on the working fluid, with options such as air-cooling or water-cooling. The air-cooling system is suitable for low-mass engines, which can dissipate excess heating energy by utilizing fins as an extended surface. Fins can absorb heat from the hot wall through conduction heat transfer and then release it to the air through convective heat transfer. Therefore, it is crucial to study fin efficiency. Many researchers have considered the impact of fin properties like material, shape, and weight and surrounding properties such as flow velocity, humidity, and temperature on the dissipation of wasted energy through conductive and convective mechanisms. Sandip and Sunilkumar [1] studied an actual engine's heat transfer using experimental and numerical methods. They examined circular fins with rectangular and triangular cross-sections, measuring the heat transfer coefficient and surface temperature distribution across a wide range of velocities. Ultimately, their findings indicated that the circular fin with a rectangular cross-section exhibited a higher heat transfer coefficient than the triangular shape. However, the surface temperature of the triangular cross-section was found to be higher than that of the rectangular type. Basim et al. [2] found that setting circular pins on the fin surface and creating curvature on the contact surface between the fin and hot wall increased the Nusselt number by approximately 30% and reduced the hot wall temperature by around 20 degrees Celsius. Additionally, Zaidshah and Yadav [3] examined heat transfer in a fin by incorporating grooves and cavities on its surface. Their study revealed that these modifications resulted in increased surface area and fluid interaction, ultimately leading to improvements in heat transfer and an increase in pressure drop. Afterward, Tariq et al. [4] examined the impact of grooves and holes on the fin surfaces using numerical and experimental methods. The research findings indicate that grooves can enhance heat transfer by approximately 40% and reduce the weight of the fins. In numerical studies, P. Prasad and L. Prasad [5] found that the zigzag shape of fins can increase heat transfer more effectively than rectangular fins by comparing the rectangular and crinkle shapes of group fins. In a study on complex fins, Hashem-ol-Hosseini et al [6] researched the distance optimization between rectangular fins in oval tube heat exchangers. They found that oval tubes are more efficient than rectangular tubes. In addition, they stated that a decrease in fin spacing leads to an increase in pressure drop. Shadlaghani et al. [7] also considered the

*Corresponding author's email: mpourjafargholi@gmail.com

heat transfer of rectangular, trapezoidal, and triangular fins through numerical analysis. They attempted to optimize the fin shape based on maximum heat transfer by assuming constant volume. The results showed that for fins with the same base, the triangular fin provided a higher heat transfer rate than the others. Additionally, it was found that increasing the height/thickness ratio of the triangular fin can enhance the heat transfer rate. Afterward, using a numerical method, Jalili et al. [8] considered the impact of installing a rectangular fin inside a tube in a tube heat exchanger. They demonstrated that the fin can enhance heat transfer rate, but has no significant effect on pressure drop. Also, Ali and Kherde [9] studied the heat transfer rate from the engine cylinder through the fins. They discovered that the contact time for the airflow and the generation of the flow of turbulence over the fin are crucial parameters in increasing the rate of fin heat transfer. Finally, they investigated the main parameters such as the effect of the fin shape, air velocity, and flow turbulence on the heat dissipation rate. After that, I. Satyanarayana and G. Pranay [10] considered the cooling of the cylinder engine by using rectangular and triangular fins. The comparison of results led to the finding that the configuration with triangular fins dissipates more heat than a rectangular fin of the same mass. In this research field, R. Vijayakumar et al. [11] also studied the heat transfer of rectangular fins and ultimately suggested an appropriate fin shape using numerical methods.

Since aluminum has a high conductivity coefficient and is lightweight, P. K. Singh et al. [12] conducted a numerical study on heat transfer using aluminum alloy fins. They introduced this metal as a practical and useful material for constructing fins. In their study, S. Durgam et al. [13] investigated the impact of the material used for heat dissipation fins in this field. They utilized ANSYS FLUENT software to compare the performance of rectangular fins made from various materials. Since fin geometry significantly affects conductive, convective, and radiative heat transfer mechanisms, another group of researchers considered the impact of fin geometry. For example, S. Mirapalli and P. Kishore [14] analyzed heat transfer dissipation from the engine using triangular fins as coolants. They also proposed the triangular fin as a new shape that could be used instead of the traditional rectangular fin. The results indicated that although triangular fins have a higher heat transfer coefficient, rectangular fins are more efficient despite their greater weight. Also, Torabi et al. [15] examined the heat transfer characteristics of rectangular, trapezoidal, and concave parabolic fins using an analytical method. They discovered that assuming the heat transfer coefficient as a function of surface temperature results in improved fin efficiency. Furthermore, they noted that increasing the conductivity factor within the fin can also enhance fin efficiency. Afterward, R. Karvinen and T. Karvinen [16] examined the heat transfer of the same geometry. They optimized the geometry based on the maximum heat flux for a constant fin volume adjacent to laminar and turbulent flow.

Finally, the summary of the recent studies mentioned is provided in Table. 1.

Table 1. The summary reviews of recent related researchs (Continued)

Researchers	Considered issue	Variable ranges	method	results
B. Freegah et al.	HTC of plate-fin heat sinks with fillet profile	Q''=18750 (W/m^2) $\dot{m}_{air}$=0.00092-0.00218-0.0033-0.00433 (Kg/s)	numerical	Enhance HTC
S. Zaidshah and V. Yadav	effect of grove and cavity on HTC of fin surface- a review	-	numerical	Enhance HTC and pressure drop rate
A. Tariq et al.	effect of groves and holes on the fin surfaces	Q=7 (W) V_{air}=8 (m/s)	Experimental and Numerical	Enhancing HTC by almost 25% Reducing weight by about 38%
P.Prasad and L.S.V Prasad	analysis HTC on louvered rectangular fin	Q''=35657 (W/m^2) V_{air}=1.41 (m/s)	numerical	Enhancing HTC by about 49% in comparison to rectangular fin

Table 1. The summary reviews of recent related researchs (Continued)

Researchers	Considered issue	Variable ranges	method	results
Hashem Alhoseini et al.	analysis HTC on the finned oval tube at different fin configure durations	Q=266 (W) V_{air}=4-8-12 (m/s)	Experimental and Numerical	More efficiency in oval fin compared to rectangular, Optimization of the distance, Increase pressure drop by space reducing
B. Jalili et al.	HTC of novel usage of the curved rectangular fin	$T_{hot\ fluid}$=50 (°C) $T_{cold\ fluid}$=25 (°C) Re=9000–21000	Numerical	Heat exchangers with a curved fin have 4% better efficiency than rectangular-type
Ali and Kherde	studied the HTC rate from the engine cylinder by the fins- a review	-	-	Introduced flow contact time and turbulency as a main parameter for HTC increasing Introduce
I. Satyanarayana and G. Pranay (2016)	considered the HTC of cylinder engine by using rectangular and triangular fins	$T\ wall$=220 (°C) V_{air}=40 (Km/h)	Numerical	The collection of triangular fins provided more HTC rate in comparison to rectangular
R. Vijayakumar	considered the HTC of rectangular fin	T_{wall}=300 (K) V_{air}=0-16 (m/s)	Numerical	proposed a suitable shape for the fin
P. K. Singh et al.	study about heat transfer by aluminum alloy fins	Q''=0.44188 (W/mm^2) T_{wall}=28 (°C)	Numerical	introduced Aluminium as a practical and useful material for fins constructing
S. Durgam et al.	considered the effect of the used material for heat dissipation fins	T_{wall}=300 (°C) V_{air}=2-20 (m/s)	Numerical	provided a performance of each rectangular fin consisting of different materials
M. Torabi et al.	studied HTC of rectangular, trapezoidal, and concave parabolic fins	-	Analytical	assumption of HTC coefficient as a function of temperature leads to an increase in fin efficiency
R. Karvinen and T. Karvinen	considered the HTC of the rectangular, trapezoidal, and parabolic fins	-	Analytical	Introduced the optimization method for driving the best geometry

Table 1. The summary reviews of recent related researchs

Researchers	Considered issue	Variable ranges	method	results
Sandip and Sunilkumar	investigated the HTC of the circular fin in rectangular and triangular shape cross-sections	T_{wall}=180 (°C) V_{air}=0-12 (m/s)	Experimental and Numerical	Report that the circular fin with a rectangular cross-section provided a higher HTC and lower surface temperature
A. Shadlaghani et al	considered the HTC of rectangular, trapezoidal, and triangular fins	T_{wall}=70 (°C) V_{air}=0-2 (m/s)	Numerical	show that for the same base, the triangular fin provides a higher HTC than the others
Sandhya Mirapalli and Kishore	considering the HTC in triangular and rectangular fins	-	analytical	Report the higher efficiency and lower HTC in rectangular in comparison to triangular fin

Although many researchers attempt to determine the optimal shape of fins for various conditions, the rectangular shape of fins remains the preferred choice in many industrial equipment. This preference is likely due to its simple and cost-effective manufacturing process. However, using rectangular fins can result in increased weight and pressure drop in engines, heat exchangers, and other equipment. Additionally, recent studies have not adequately explored the impact of the contact angle between the fin and cooling flow. Comprehensive research is necessary to determine the most suitable type of fins for use in lightweight engines under different conditions. In the current study, the effect of the angle at which air hits the fin surface was examined. This parameter directly influences the convective heat transfer coefficient of the fin surface but has not received sufficient attention in recent research. This study considered the angle at which the airflow hits the fin and other factors that affect fin efficiency, such as fin geometry, airflow velocity, and heat dissipation rate. An accurate and innovative experimental setup was used to analyze the impact of each parameter under various conditions.

2- Experimental Setup

The experimental investigation required the setup available to measure the effect of every parameter on the specific phenomenon. Additionally, enough information about the occurrence of mechanisms is necessary to design and fabricate a suitable setup. The heat dissipating phenomena by fins have conductive, convective, and radiative mechanisms, which have several effective parameters such as geometry, material, angle or position of the fins, coolant flow velocity, applied heat flux, wall temperature, etc. Therefore, the experimental system should be designed in such a way that it measures all these effective parameters.

In this study, a suitable setup that can change the active and passive parameters is designed and developed according to the schematic of the experimental system in Fig. 1. This setup can consider the effect of the active parameter such as fin geometry by changing the fin type, and can change the passive parameter such as air velocity or heat flux by controlling the surrounding conditions.

The process begins with the heat flux applied to the wall which is done by cartridge heaters (3). The three holes in the primary wall (2) allow the heaters to be set, while the front side of the wall is stuck to the fin (1), and the other side is insulated by an insulator (4) which consists of a fiber box filled with glass wool. The heating power was controlled by an electrical dimmer (10) and calculated by the multiplication of the value of electrical voltage and current which was measured by voltage and current meter (9).

The cooling airflow is provided by the axial fan (6) while its velocity is controlled and measured by dimmer (10) and digital anemometer (5). Additionally, the temperature at a specific point on the fin surface is measured by a PT-100 sensor (7) and displayed on a digital thermostat (8). After reaching stability, the temperature distribution, cooling velocity, and heating power can be experimentally determined by considering the geometry and angular position of the fin. The effective and measuring parameters, and the range of variation for each, are shown in Table. 2.

The heat transfer comparison between the rectangular and triangular fins was conducted under the condition where the occupied space of each fin was similar. This means that the size of each side of the square root, its area, and the length

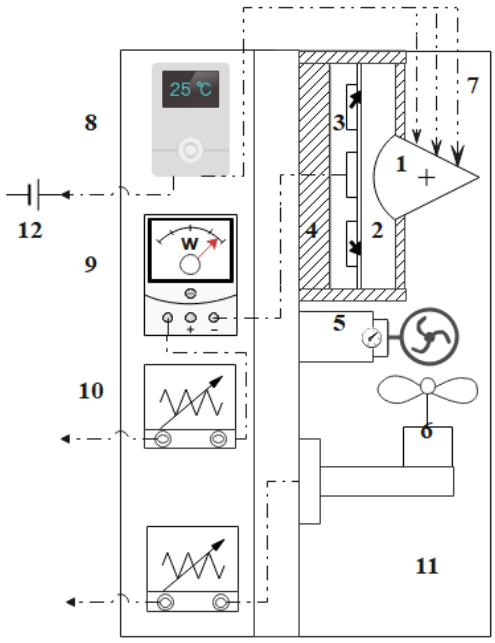

1. Fin
2. Hot Wall
3. Cartridge heater
4. Insulation
5. Anemometer
6. Fan
7. PT-100 Sensor
8. Thermostat
9. Current and Voltage Meter
10. Electrical Dimmer
11. Body
12. Power Supply

Fig. 1. The schematic of the experimental setup with measuring apparatus

Table 2. The main effective parameter and related measuring equipment

Parameters	Range of Variation	Applying Equipment	Measuring Equipment	Controlling Equipment
Heat Flux (kW/m^2)	4.6-18.5	Cartridge Heater	Digital Multi-meter	Electrical Dimmer
Air Flow Velocity (m/s)	1, 2	Axial Fan	Digital Anemometer	Electrical Dimmer
Angle Position	0, 45, 90	Angle mechanism	Protractor	manual
Air Flow Temperature (ºC)	17.5	Chiller	Chiller	Chiller control system
Surface Temperature (ºC)	-	-	PT-100 sensor	-

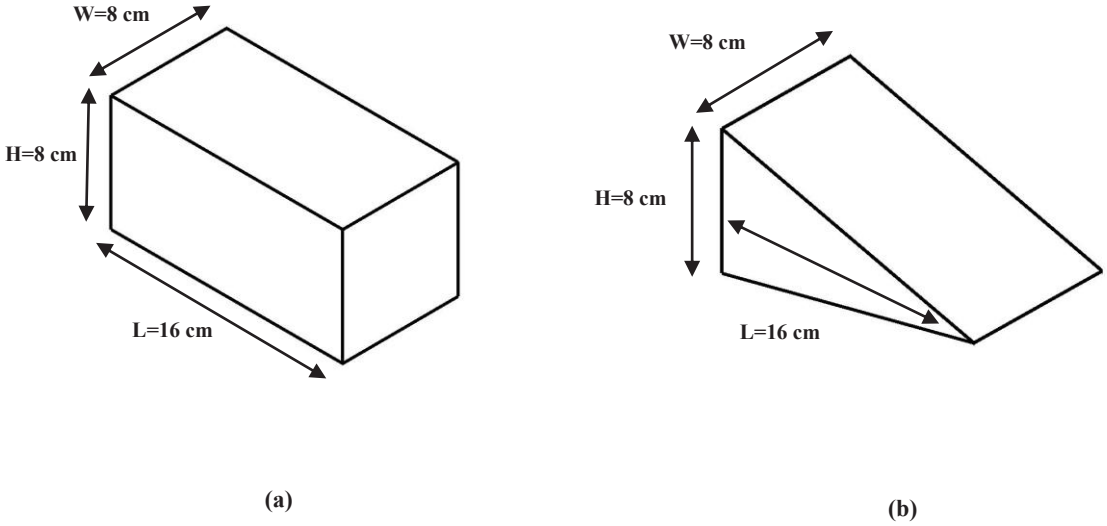

Fig. 2. The dimension value of (a) rectangular, (b) triangular fin

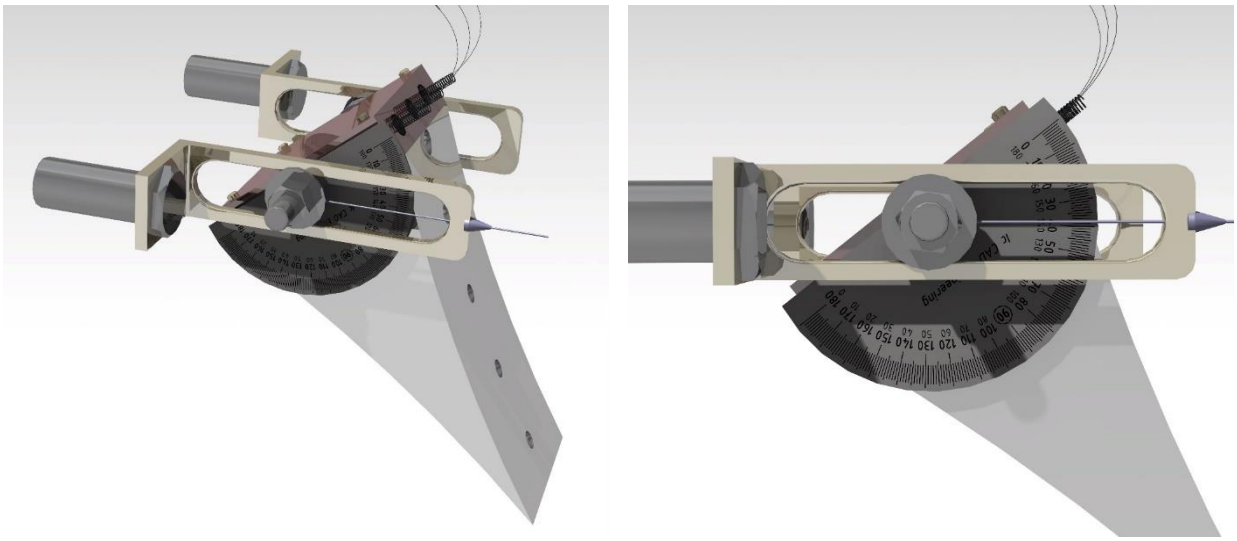

Fig. 3. The designed and fabricated mechanism for changing the angle between the fin and cooling flow direction

of each fin are equal, so the only difference between the rectangular and triangular fins lies in their geometric features. The dimensions of each side of the rectangular and triangular fins are depicted in Fig. 2.

Additionally, the mechanism was designed to adjust the angle between the fin and the flow direction, as shown in Fig. 3. This angle change mechanism includes a protractor, guidance probe, and wing nuts that allow to setting of the angle of the base plane and the attached fin. As the cooling flow only travels along the duct, any alteration in the fin angle will cause a change in the angle of impact between the fin and the flow direction.

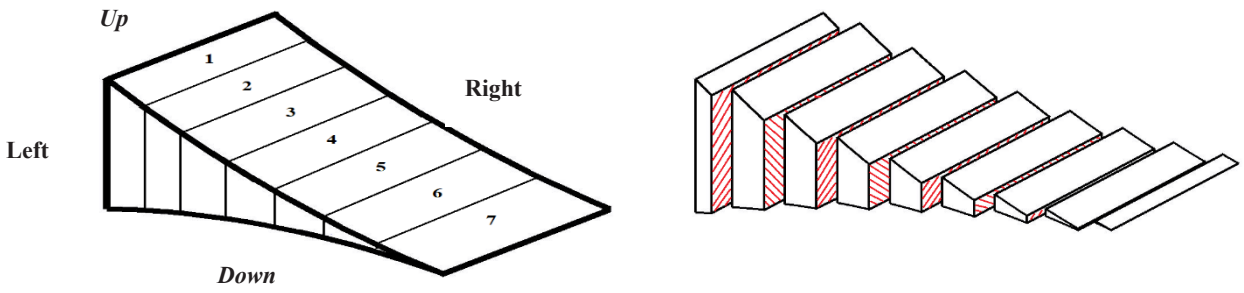

(a) (b)

Fig. 4. The schematic of the desired zone for (a) temperature measuring and (b) its related hatched cross-section area

3- The Experimental Methodology

For this study, as shown in Fig. 4, each fin is divided into seven cross sections along the length direction, and the temperature of the center and four sides of each cross section will be measured.

Therefore, the central and surface temperatures of the fin are measured to determine the temperature distribution and heat transfer coefficient on each surface. The surface temperature in the center and around each zone was measured by attaching the PT-100 sensor in different holes. additionally, the conductive heat transfer rate which transfers from the center of each zone to the surface of each side is determined according to Eq. (1) [17]

$$Q^{\bullet}{}''_{Center-Surface} = K\frac{\left(T_{Center} - T_{Surface}\big|_{each\ sides}\right)}{d} \quad (1)$$

The convective heat transfer coefficient between the zone surface and cooling flow for each side can be determined according to Eq. (2) [17]

$$h_{Each\ Side} = \frac{Q^{\bullet}{}''_{Center-Surface}}{\left(T_{Surface\ |\ Each\ Side} - T_{Fluid\ Flow}\right)} \quad (2)$$

Finally, according to Eq. (1-2), the average surface temperature distribution of the fin and the average convective heat transfer coefficient of each desired zone of the fin can be determined. Diagrams also play a significant role in comparing the mechanical or economic efficiency of different fin geometries. Following this, the pressure drop or resistance of the fin against the passing flow can be qualitatively estimated by considering the cooling flow velocity.

Additionally, the streamlines of the cooling flow were determined using Ansys-Fluent software for each flow contact angle, such as 0, 45, and 90 degrees. The streamlines for the rectangular fin are illustrated in Fig. 5.

Also, Fig. 6 shows the streamlines of the triangular fin.

4- Validation

Every experimental investigation requires validation through another similar study to prove its reliability. Meanwhile, the comparison of temperature distribution along the rectangular fin between experimental data and Hung-Tung [18] is presented in Fig. 7

According to Fig. 7, the deviation in temperature data between the experimental and Hung-Tung studies is less than 10%. Additionally, the efficiency of the rectangular and triangular fin is compared between the experimental and Mirapalli-Kishore [14] data in Fig. 8.

According to Fig. 8, the deviation of efficiency data between the present study and the Mirapalli-Kishore study is less than 20%.

It is often challenging to find studies with identical physical conditions. Additionally, comparing multiple parameters between two phenomena can be computationally costly. Therefore, using dimensionless groups can be suggested to convert many comparing parameters into a few finite groups. Also, comparing dimensionless groups of two phenomena can reduce computational and time costs. Therefore, developing dimensionless groups for the main parameters of specific phenomena allows for comparison across different conditions. In this case, the Huang-Tung

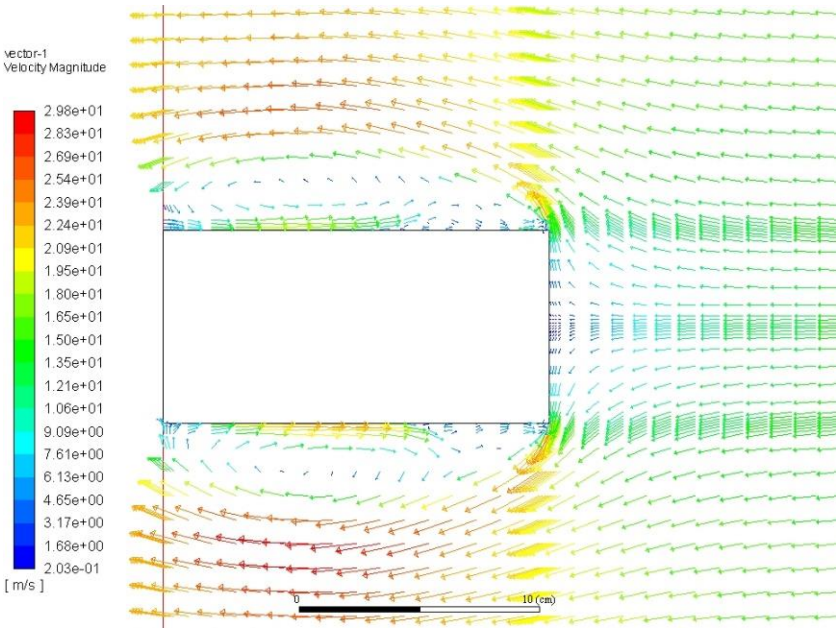

(a)

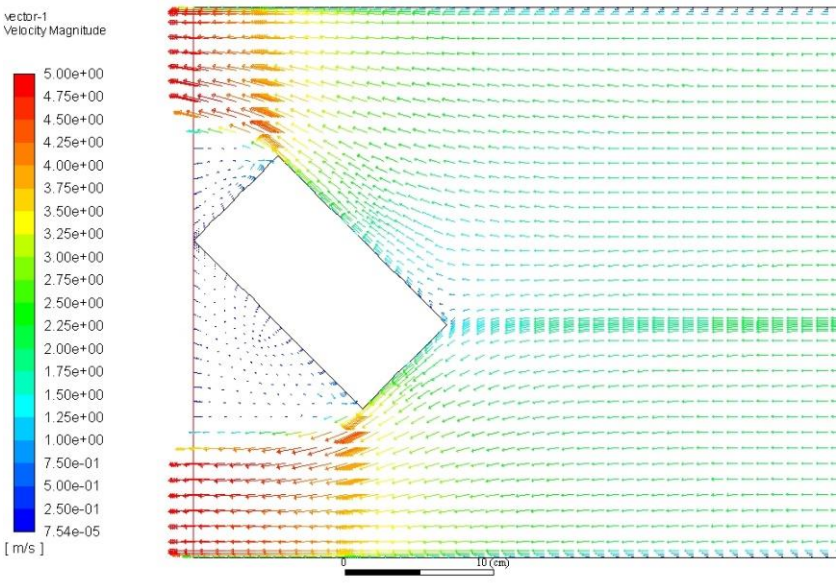

(b)

Fig. 5. The streamlines of cooling flow in contact by a rectangular fin in (a) 0, (b) 45, and (c) 90 degree (Continued)

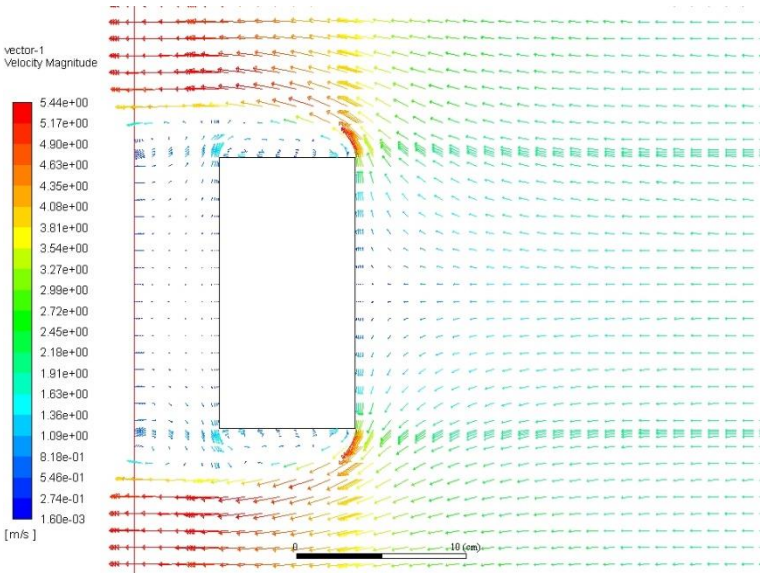

(c)

Fig. 5. The streamlines of cooling flow in contact by a rectangular fin in (a) 0, (b) 45, and (c) 90 degree

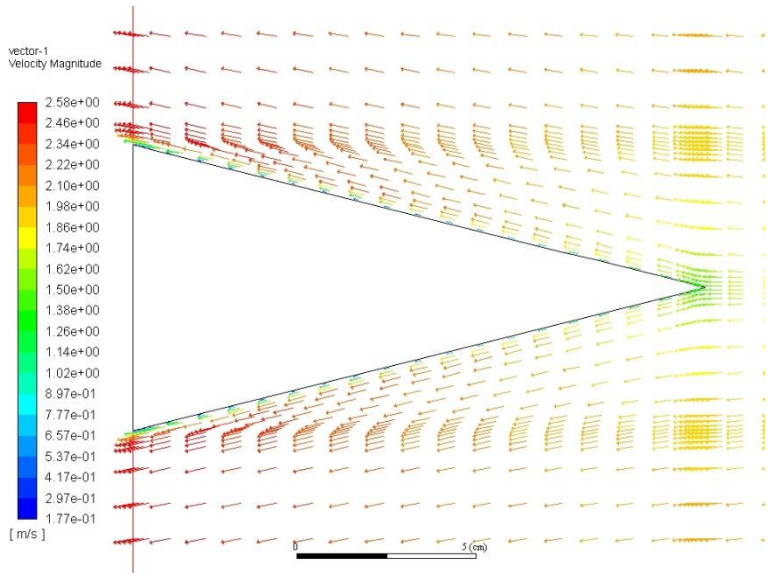

(a)

Fig. 6. The streamlines of cooling flow in contact by a triangular fin in (a) 0, (b) 45, and (c) 90 degree (Continued)

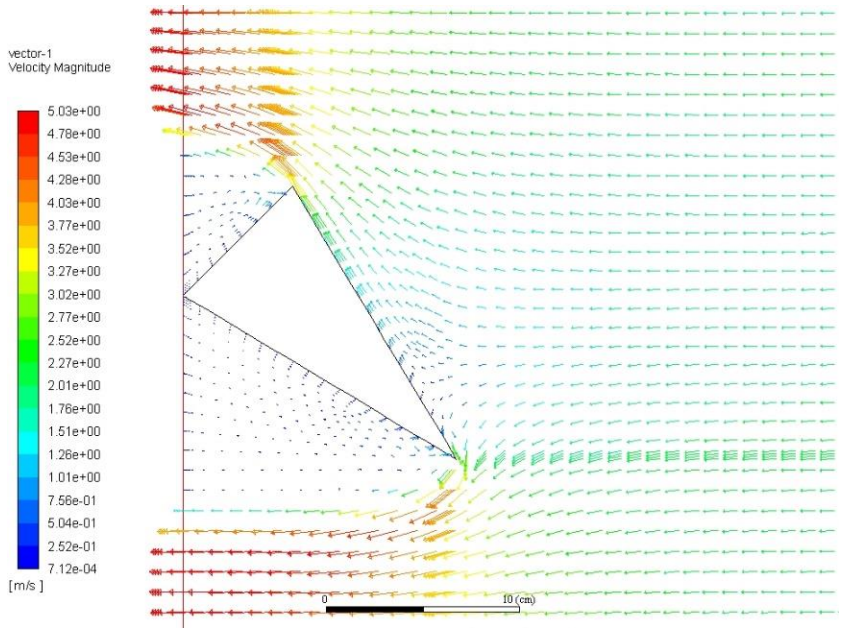

(b)

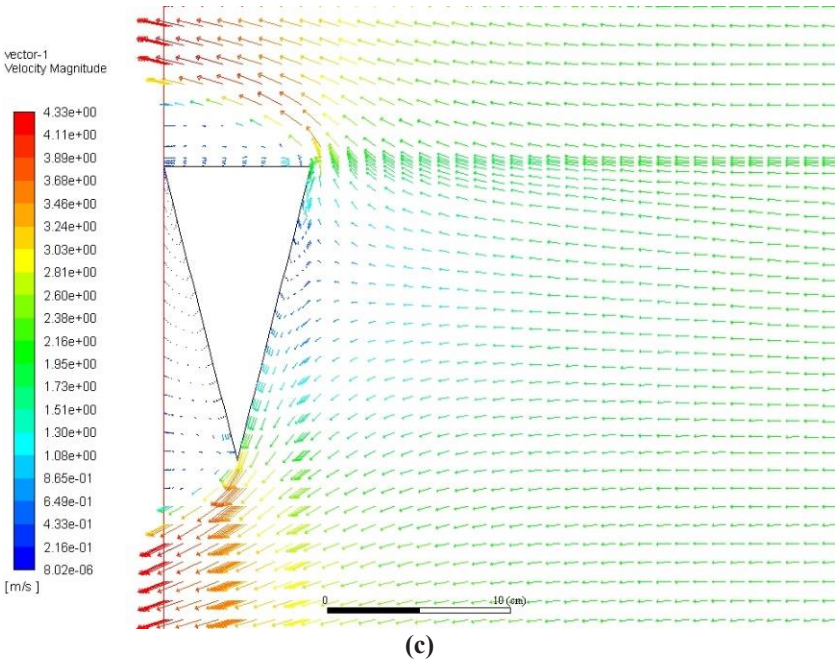

(c)

Fig. 6. The streamlines of cooling flow in contact by a triangular fin in (a) 0, (b) 45, and (c) 90 degree

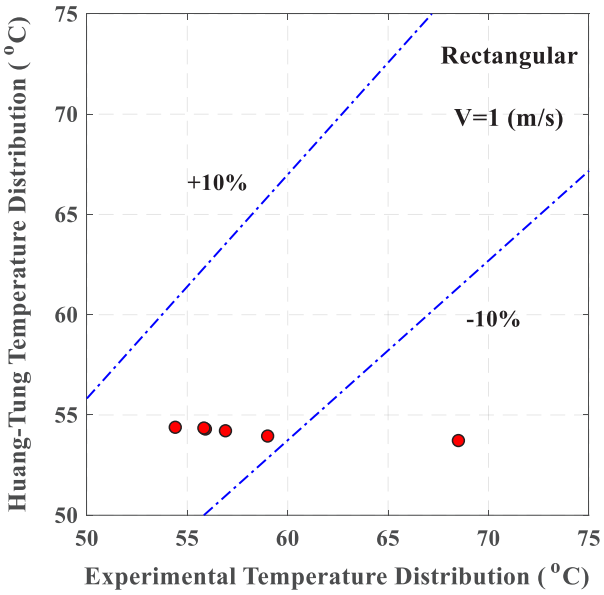

Fig. 7. the comparison of temperature distribution between the present study and the Hung-Tung study

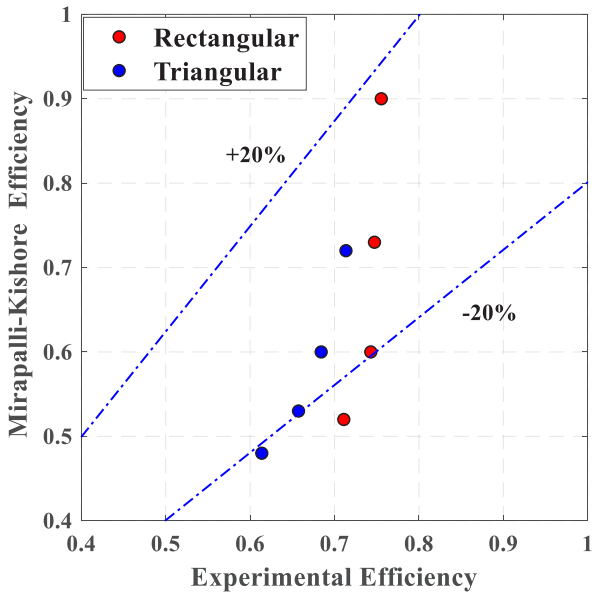

Fig. 8. the comparison of the efficiency between the present experimental and the Mirapalli-Kishore study

Table 3. The main effective parameter and related dimensionless group for Huang-Tung and the present research

	Q (W)	V (m/s)	L (m)	A (m^2)	T_r (ºC)	Π_1	Π_2	Π_3	Ψ
Huang-Tung	4	1.5	0.055	0.00015	50.5	43075.2	6584.4	0.04959	0.14064
Experiment	118.3	1.8	0.16	0.0064	112.8	22162.2	2641.2	0.25	0.14634

study was chosen for validation using dimensionless groups [Appendix A] established by the Pi-Buckingham theorem [19] as shown in Eq. (3-6).

$$\Pi_1 = \frac{T_r K_s}{\rho_f V^3 L} \tag{3}$$

$$\Pi_2 = \frac{Q''}{\rho_f V^3} \tag{4}$$

$$\Pi_3 = \frac{A_c}{L^2} \tag{5}$$

$$\Psi = \Pi_1 * \Pi_2 * \Pi_3 * 10^{-8} \tag{6}$$

These dimensionless groups enable comparability between different experiments. For this validation, combining groups creates a new dimensionless group that considers important parameters such as velocity, root zone temperature, heat flux, length, and cross-sectional area of each fin. The results of the Huang-Tung [18] study and the present research are presented with related dimensionless group values in Table. 3.

According to Table. 3, a comparison of the dimensionless groups' multiplication in the Huang-Tang study and the present research demonstrates the high accuracy of the measured data by the manufactured experimental system.

5- Results and Discussions

In this section, we will discuss the impact of effective parameters on fin heat transfer characteristics, using the range of variation provided in Table. 2. Additionally, we will illustrate the heat transfer coefficient, temperature distribution, and pressure drop results.

5- 1- Heat Transfer Coefficient

In this study, the convective heat transfer coefficient for each side of the rectangular and triangular fin was calculated. The superficial and central temperatures along the fin were measured for each 2-centimeter distance. Finally, the heat flux and HTC were calculated for the surfaces at the top, bottom, left, and right sides using Equations 1 and 2.

5- 1- 1- HTC for Rectangular Fin

The heat transfer coefficients (HTC) for each side of the rectangular fin were calculated for different conditions and angles of 0, 45, and 90 degrees. In this section, the HTC for the angle of 0 degrees between the flow direction and fin for different conditions is illustrated in Fig. 9.

According to Fig. 9, the HTC curve on the surface of the left, right, top, and bottom sides of the fins shows a zigzag pattern, which may be caused by the flow pattern at the impact point on the fin. In other words, when the cooling flow reaches the tip of the fin, it must jump to pass over it. This jumping action causes the cooling flow to stagnate at the fin surface. This phenomenon could be considered as the main reason for the decrease in HTC in the region near the end of the fin.

According to the streamline direction provided in Fig. 5, for a rectangular fin in the θ=0 or parallel position, once the cooling flow reaches the end of the fin, the high flow velocity and low temperature can result in a high heat transfer coefficient in this zone. Shortly after, due to the square tip of the rectangular fin as shown in Fig. 2, the crossing flow must pass over the fin, causing vorticity and backward flow. This creates a stagnation zone and begins to reduce the heat transfer coefficient. Further along, the flow reattaches to the fin surface, increasing the heat transfer coefficient. Finally, after these phenomena occur at the base of the fin, a dead zone is created, leading to a decrease in the heat transfer coefficient. Therefore, based on the provided Figure, the zigzag behavior observed in HTC Figures related to rectangular fins is significant. It is noted that the vortices created by the tip on each side can interact, potentially impacting the heat transfer mechanism at the end of the fin.

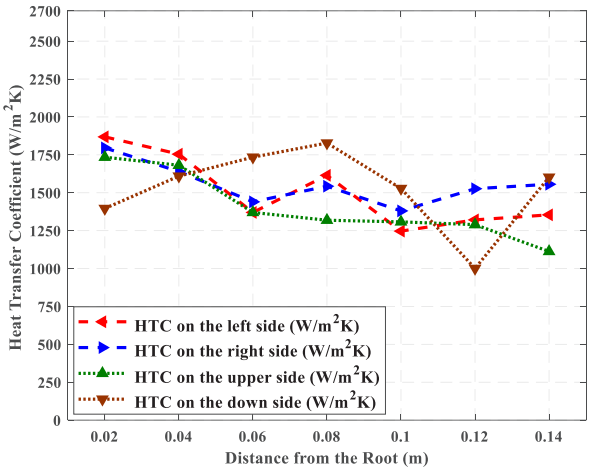

(a) Q''=18.5 (kW/m2), V=2.14 (m/s), θ=0º, T_f=17.45 (ºC)

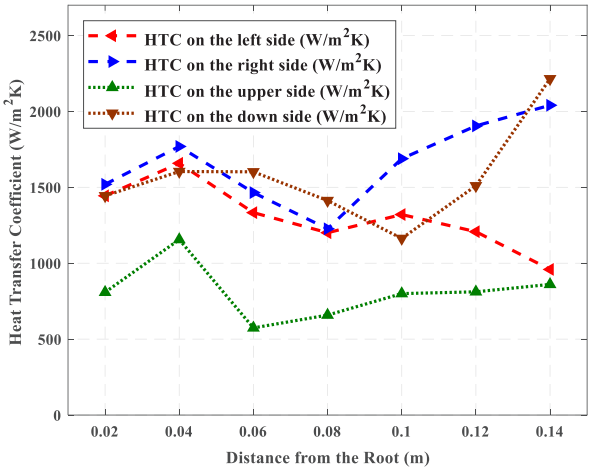

(b) Q''=18.5 (kW/m2), V=1 (m/s), θ=0º, T_f=17.1 (ºC)

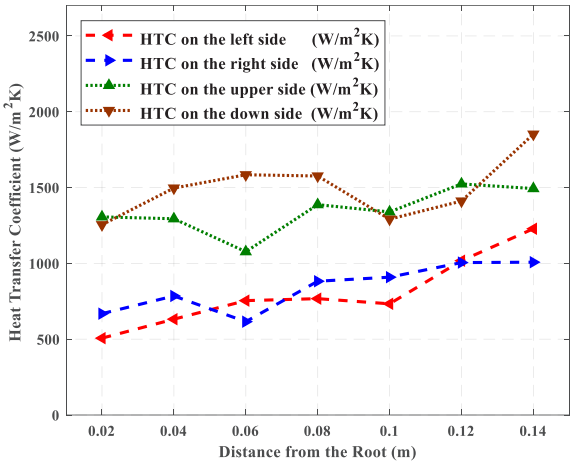

(c) Q''=4.6 (kW/m2), V=2.08 (m/s), θ=0º, T_f=17.4 (ºC)

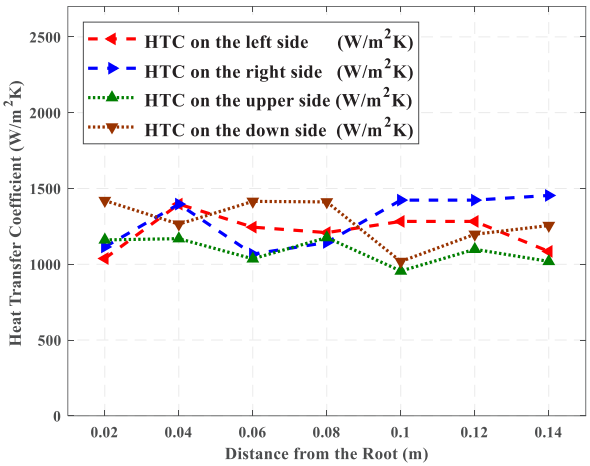

(d) Q''=4.6 (kW/m2), V=1 (m/s), θ=0º, T_f=17.85 (ºC)

Fig. 9. The HTC for each side of the rectangular fin in different conditions

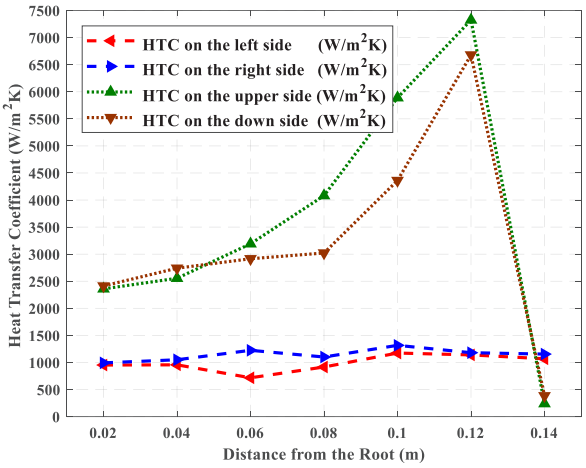

(a) Q''=18.5 (kW/m^2), V=2.36 (m/s), θ=0º, T_f=15.83 (ºC)

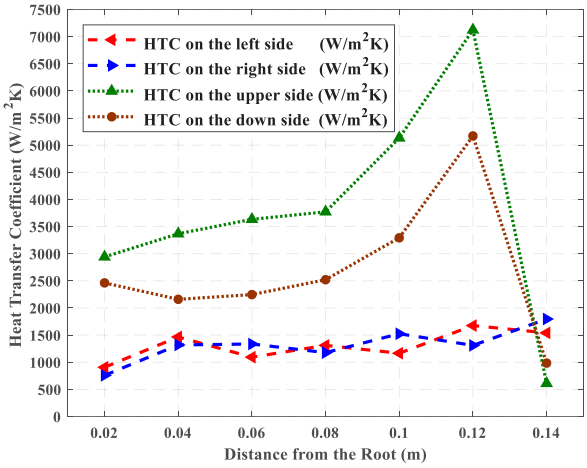

(b) Q''=18.5 (kW/m^2), V=1 (m/s), θ=0º, T_f=20.7 (ºC)

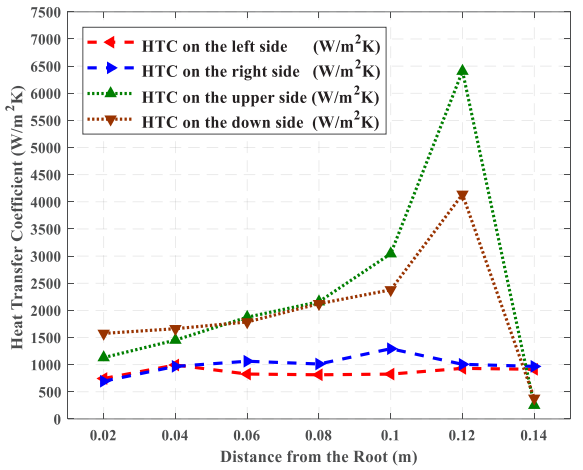

(c) Q''=4.6 (kW/m^2), V=2.35 (m/s), θ=0º, T_f=17.45 (ºC)

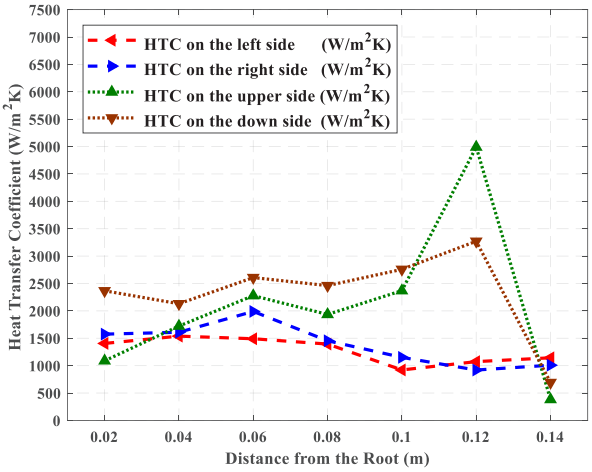

(d) Q''=4.6 (kW/m^2), V=1 (m/s), θ=0º, T_f=18.9 (ºC)

Fig. 10. The HTC for each side of the triangular fin in different conditions

In other words, due to variations in vorticity levels on each side of the rectangular fin and the resulting interactions, the extent of zigzag behavior on each side may differ.

5- 1- 2- The HTC for Triangular Fin

The results of the HTC for a triangular fin under various conditions, with the fin and cooling flow direction parallel to each other, are shown in Fig. 10.

Like the rectangular fin, the sharp geometry of the triangular fin can reduce many of the vorticity or stagnation phenomena by cooling flow. Additionally, the distance between the center and the surface of the triangular fin is not equal. In other words, the distance between the upper or bottom surface and the central line reduces linearly, while the distance from the left or right surface of the central line remains constant along the fin. Thus, the heat transfer coefficient (HTC) along the upper and bottom sides of the triangular fin has a greater difference than the other sides.

The temperature at the center, upper, and bottom sides of the triangular fin in the tip region approximately has the same value.

Moreover, the very tiny cross-section at the tip can cause very low heat transfer. Therefore, the HTC at the top and bottom sides of the triangular fin is very low, but it can increase after flow passes from the tip due to the increased heating surface or superficial heat flux. After that, from the end region to the root, the HTC decreases similarly to a rectangular fin.

The HTC curve at the left or right surface has the same behavior as a rectangular fin, with the zigzag behavior not seen, likely due to removing the vorticities with the sharp tip.

According to Fig. 2 and 6, the triangular fin has four sides in the up, down, left, and right directions. The thickness of the fin in the up and down direction decreases linearly along the fin. The heat transfer coefficient in the upper and lower surfaces is negligible due to the small tip and very low-temperature gradient or heat flux. A short distance after that, the surface area increases, and the heat transfer coefficient grows significantly, similar to a rectangular fin. Additionally, the sharp tip in triangular geometry can eliminate vortices and their effects, such as zigzag behavior in the heat transfer coefficient curve.

Finally, from the terminal areas of the fin to the base, the heat transfer coefficient decreases smoothly due to the fluid flow temperature increasing in the boundary layer. The thickness of the fin remains constant in the left or right direction like a rectangular fin, while the effect of vortices on these side surfaces is minimal, and the heat transfer behavior of these surfaces is similar to a rectangular fin, with a very brief zigzag behavior.

5- 2- HTC comparison

The average heat transfer for each 2-centimeter distance along the rectangular and triangular fins, when positioned parallel to each other (0 degrees), was determined. The average heat transfer coefficient (HTC) comparison between the rectangular and triangular fins in the parallel position (0 degrees) is illustrated in Fig. 11.

According to the results of section 5.1, it was found that the sharp tip of the triangular fin can significantly reduce vorticity or flow stagnation, while the square tip of the rectangular fin forces the flow to jump, causing stagnation [20]. This phenomenon results in a notable reduction in HTC along the rectangular fin compared to the triangular fin, as shown in Fig. 11.

5- 3- Dimensionless Heat Transfer

In addition to convective heat transfer (HTC), conductive heat transfer also has a significant effect on heat dissipation from the wall. Therefore, according to Eq. (7) [17], the dimensionless number based on the ratio between convective heat transfer on the fin surface and conductive heat transfer into the structure was introduced.

$$\frac{Q''_{Convective}}{Q''_{Conductive}} = \frac{h_{ave.}\left(T_{Surf.} - T_{Fluid}\right)}{\frac{K}{y}\left(T_{Center} - T_{Surf.}\right)} = 1 \Rightarrow \quad \frac{h_{ave}\, y}{K} = \frac{T_{Center} - T_{Surf.}}{T_{Surf.} - T_{Fluid}} = Nu^* \tag{7}$$

Nu^* of the rectangular and triangular fins is compared for θ=0 degrees in Fig. 12. As seen in this figure, Nu^* of the rectangular fins is higher than that of the triangular fin, while the rectangular fin has a lower HTC than the triangular fin. According to Eq. (7), this means that the rectangular fins provide stronger conductive heat transfer compared to the triangular fin.

Additionally, according to Fig. 2, the length, width, height, and all sides of the base of the rectangular and triangular fins have the same value. Also, no surface of these fins is insulated. Thus, the heating surface of the rectangular fin is about 76 percent larger than the triangular fin, allowing it to dissipate more heating energy to the ambient.

5- 4- Temperature Distribution

The temperature distribution along the fin is considered one of the main parameters to evaluate fin efficiency. By focusing on specific regions within each fin for this study, the average surface temperature every 2 centimeters along the rectangular and triangular fins is provided in Fig. 13. Surface temperature distribution along the fin is a key parameter for comparison with an ideal fin; a constant temperature distribution along the fin represents an ideal fin. Therefore, if the temperature distribution curve along the fin resembles a constant line, the fin is considered highly efficient. According to Fig. 13, the temperature distribution curve along the rectangular fin is closer to a constant line compared to the triangular fin, indicating higher efficiency in the rectangular fin.

In addition, the root or wall temperature of each fin was measured using the PT-100 sensor. The related results are presented in Table. 4 for different conditions. According to the results, the average temperature of the root for the triangular fin is about 44% higher than that of the rectangular type.

According to Table. 4, the mean root temperature of rectangular fins is 94°C, while for triangular fins it is 135°C under different experimental conditions.

5- 5- Dimensionless Temperature

After analyzing the temperature distribution, it became clear that the temperature at the wall, as well as the fluid flow, plays a more significant role in evaluating the efficiency of the fin. Therefore, for this study, a dimensionless temperature parameter was introduced as per Eq. (8) [17].

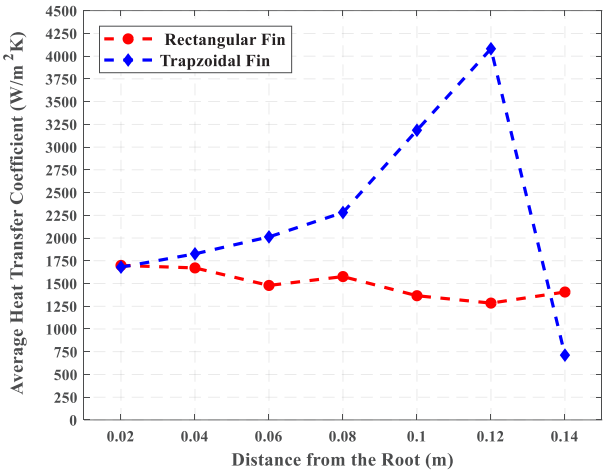

(a) Q''=18.5 (kW/m^2), V=2.25 (m/s), θ=0º, T_f=16.64 (ºC)

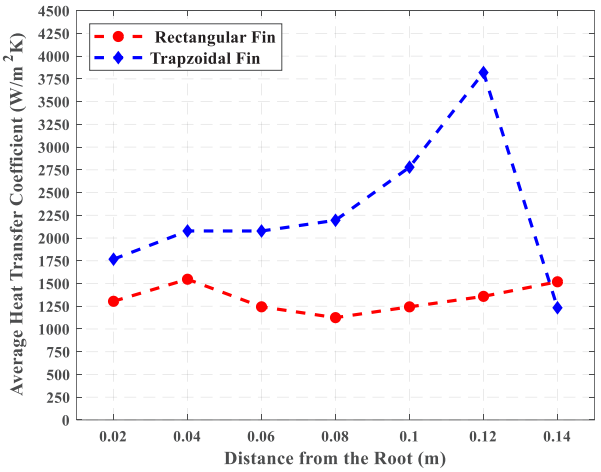

(b) Q''=4.6 (kW/m^2), V=2.21 (m/s), θ=0º, T_f=19.05 (ºC)

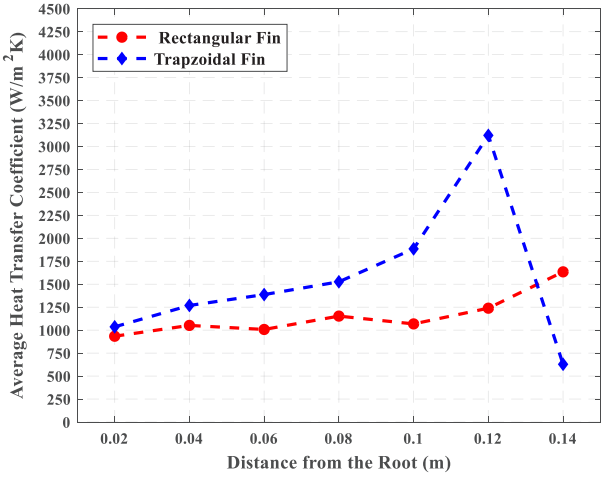

(c) Q''=18.5 (kW/m^2), V=1 (m/s), θ=0º, T_f=18.9 (ºC)

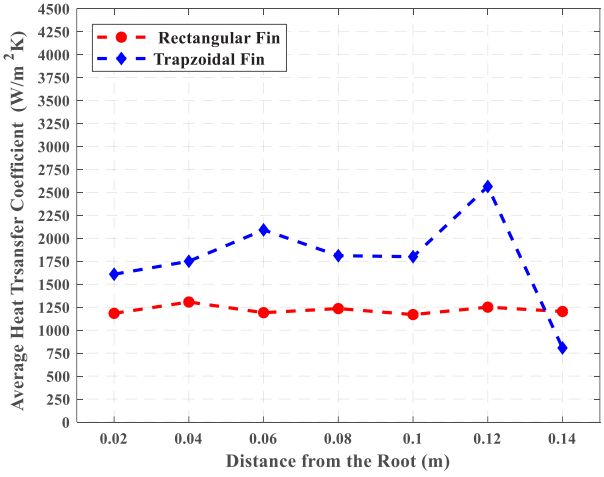

(d) Q''=4.6 (kW/m2), V=1 (m/s), θ=0º, T_f=18.38 (ºC)

Fig. 11. The average heat transfer coefficient in rectangular and triangular fins in different conditions

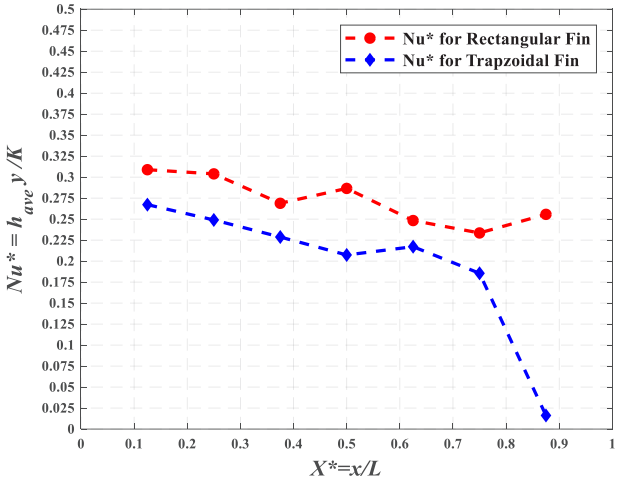

(a) Q''=18.5 (kW/m^2), V=2.25 (m/s), θ=0º, T_f=16.64 (ºC)

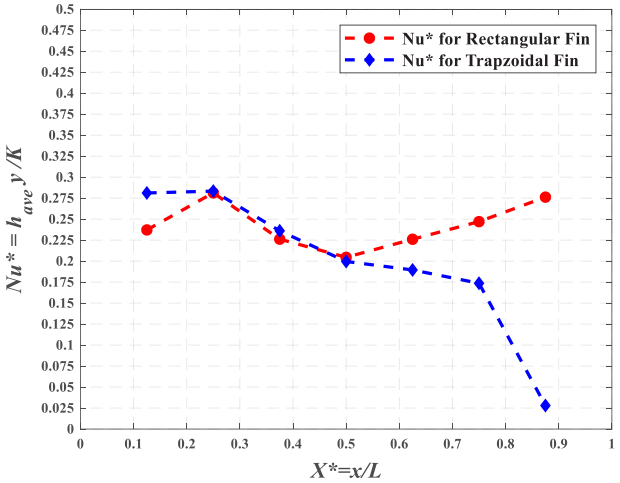

(b) Q''=4.6 (kW/m^2), V=2.21 (m/s), θ=0º, T_f=19.05 (ºC)

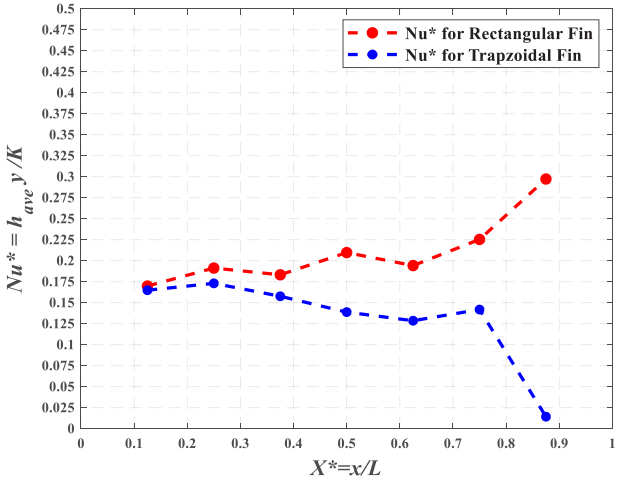

(c) Q''=18.5 (kW/m^2), V=1 (m/s), θ=0º, T_f=18.9 (ºC)

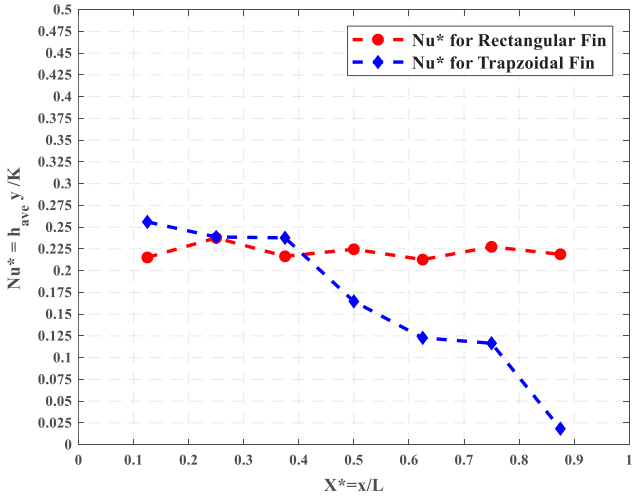

(d) Q''=4.6 (kW/m^2), V=1 (m/s), θ=0º, T_f=18.38 (ºC)

Fig. 12. The Nu* for rectangular and triangular fin in different conditions

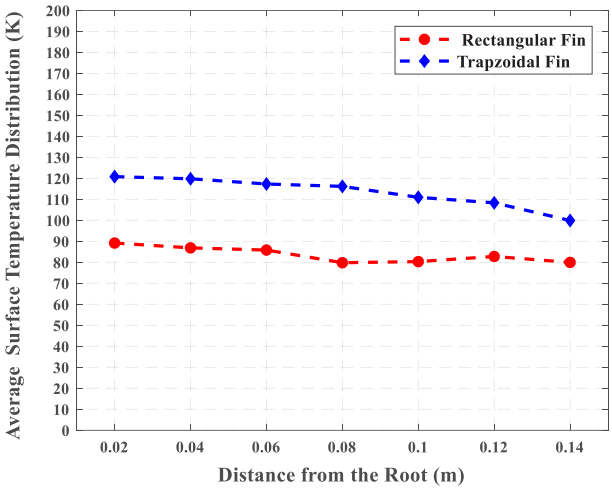

(a) Q''=18.5 (kW/m^2), V=2.25 (m/s), θ=0º, T_f=16.64 (ºC)

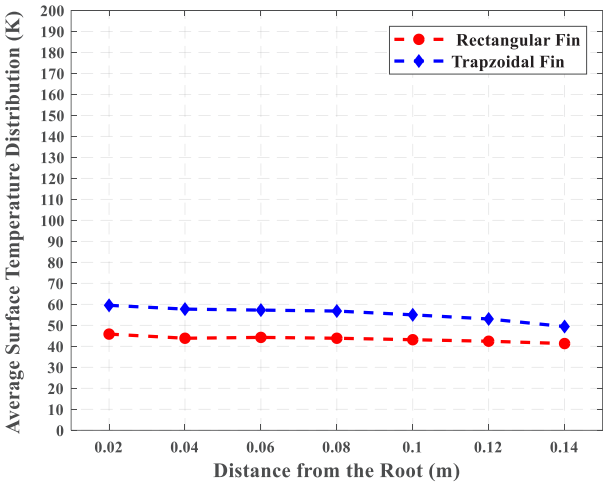

(b) Q''=4.6 (kW/m^2), V=2.21 (m/s), θ=0º, T_f=19.05 (ºC)

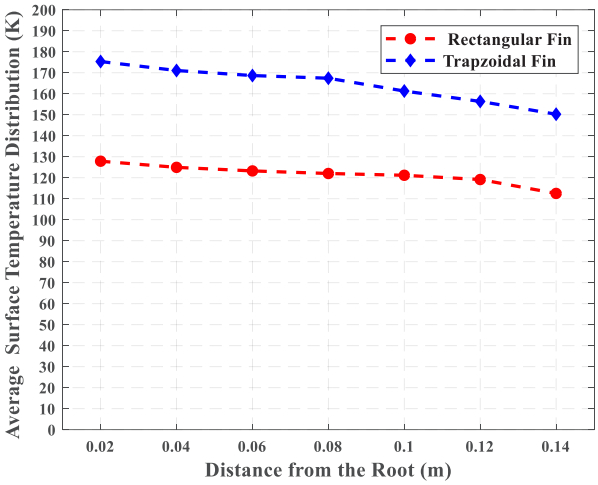

(c) Q''=18.5 (kW/m^2), V=1 (m/s), θ=0º, T_f=18.9 (ºC)

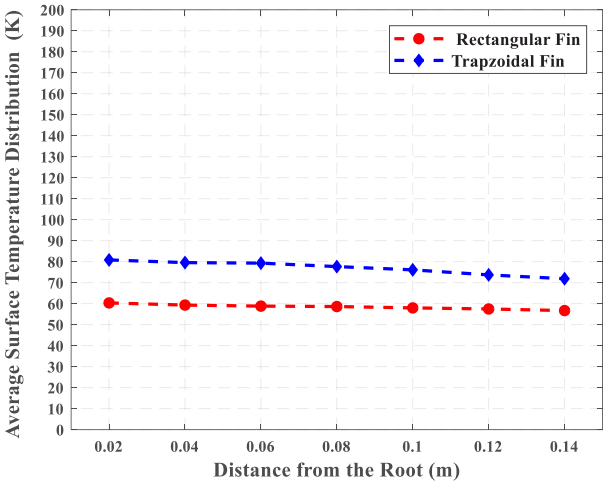

(d) Q''=4.6 (kW/m^2), V=1 (m/s), θ=0º, T_f=18.38 (ºC)

Fig. 13. The average surface temperature in rectangular and triangular fins in different conditions

Table 4. The root temperature of the rectangular and triangular fin in different conditions

Type	Heat Flux (kW/m^2)	Velocity (m/s)	Angle (degree)	T_w (°C)
Rectangular	18.5	1	90	141
Rectangular	4.6	1	90	68.5
Rectangular	18.5	1.8	90	112.8
Rectangular	4.6	1.8	90	55
Rectangular	18.5	2.2	45	107
Rectangular	4.6	2.08	45	56
Rectangular	4.6	1	45	70
Rectangular	18.5	1	45	139
Rectangular	18.5	2.14	0	106
Rectangular	4.6	2.08	0	53.8
Rectangular	18.5	1	0	147.4
Rectangular	4.6	1	0	69.8
Triangular	18.5	2	90	158.6
Triangular	4.6	2	90	76
Triangular	18.5	1	90	211
Triangular	4.6	1	90	95
Triangular	18.5	1.4	45	171
Triangular	4.6	1.4	45	77.5
Triangular	18.5	1	45	184.5
Triangular	4.6	1	45	89.5
Triangular	18.5	2.36	0	166.5
Triangular	4.6	2.36	0	75.7
Triangular	18.5	1	0	216.2
Triangular	4.6	1	0	98.9

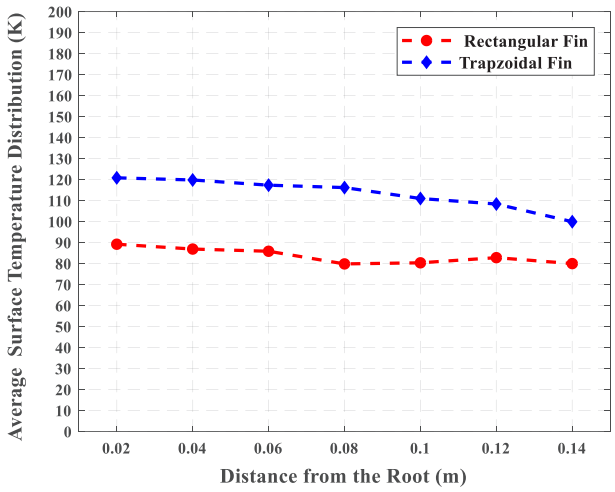

(a) Q''=18.5 (kW/m^2), V=2.25 (m/s), θ=0º, T_f=16.64 (ºC)

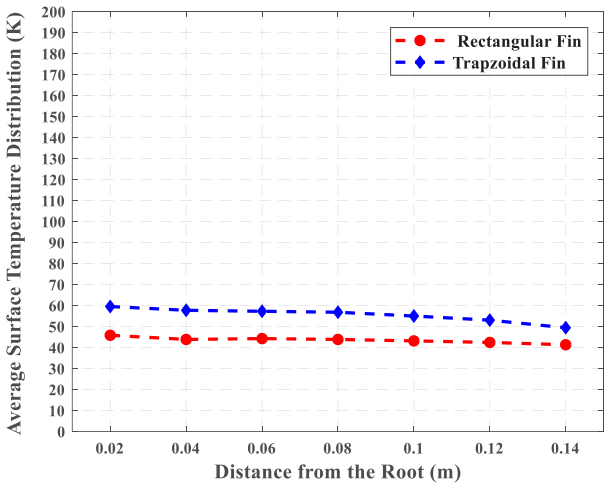

(b) Q''=4.6 (kW/m^2), V=2.21 (m/s), θ=0º, T_f=19.05 (ºC)

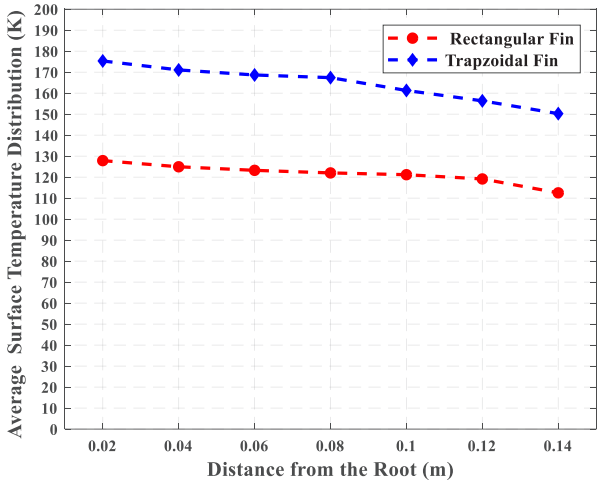

(c) Q''=18.5 (kW/m^2), V=1 (m/s), θ=0º, T_f=18.9 (ºC)

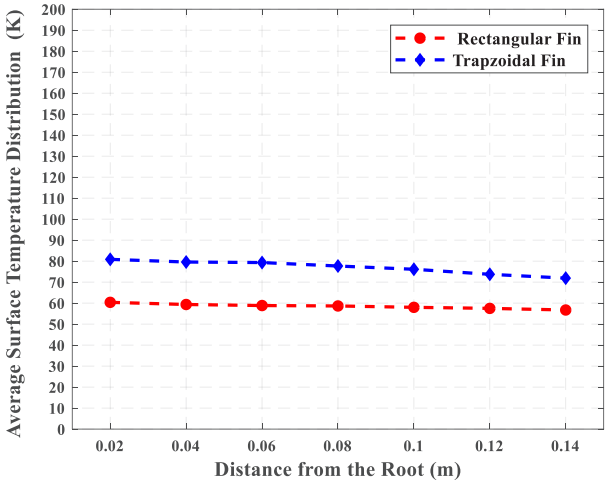

(d) Q''=4.6 (kW/m^2), V=1 (m/s), θ=0º, T_f=18.38 (ºC)

Fig. 14. The dimensionless temperature in rectangular and triangular fins in different conditions

$$\theta = \frac{T_s - T_f}{T_w - T_f} \tag{8}$$

Fig. 14 illustrates the dimensionless temperature versus dimensionless length along the rectangular and triangular fins. It is important to note that the surface temperature used in Eq. (8) and Fig. 13-14 is the average surface temperature of the upper, lower, left, and right sides of the fins.

The comparison of the dimensionless temperature distribution between rectangular and triangular geometries versus the dimensionless length of the fins is illustrated in Fig. 14. In this comparison, the wall and cooling fluid temperatures were considered for each case. According to Fig. 14, the dimensionless temperature distribution of the rectangular fin is close to the unique line related to the wall temperature. This could be due to the temperature along the rectangular fin being closer to the wall temperature. Therefore, it can be concluded that the efficiency of the rectangular fin may be higher than that of the triangular type.

Table 5. The root temperature of the rectangular and triangular fin in different conditions

Type	Wall Heat Flux (W/m^2)	Velocity (m/s)	$h_{ave.}$ (W/m^{2}K)	Θ degree	η
Rectangular	18491	1	1087	90	0.7912
	4622	1	1083	90	0.7697
	18491	1.8	1266	90	0.7371
	4622	1.79	1357	90	0.7754
	18491	2.2	1418	45	0.7395
	4595	2.08	1516	45	0.7
	4622	1	1109	45	0.7784
	18382	1	1081	45	0.8164
	18491	2.14	1497	0	0.7462
	4595	2.08	1334	0	0.836
	18382	1	1156	0	0.7838
	4595	1	1220	0	0.7787
Triangular	18382.35	1.97	1885.98	90	0.691222
	4622.781	2	2004.593	90	0.679063
	18491.12	1	1648.878	90	0.784521
	4595.588	1	1917.748	90	0.752147
	18491.12	1.4	1698.482	45	0.623427
	4595.588	1.4	2003.184	45	0.63301
	18382.35	1	1575.535	45	0.728826
	4595.588	1	1691.051	45	0.718314
	18491.12	2.36	2253.978	0	0.671418
	4568.713	2.35	2278.459	0	0.64606
	18491.12	1	1550.595	0	0.727894
	4622.781	1	1775.997	0	0.72593

5- 6- Efficiency

In a real fin, the temperature distribution along the fin decreases as you move along its length. In contrast, the temperature in an ideal fin remains constant and equal to the wall temperature. Based on the results of sections 5.4 and 5.5, the surface temperature of an ideal fin is equal to the wall temperature. Therefore, the ratio between the heat transfer of a real fin and an ideal fin is determined by the efficiency factor introduced in Eq. (9) [17].

$$\eta = \frac{Q_{real}}{Q_{ideal}} = \frac{h_{ave.}\left(T_{surf.|ave.} - T_f\right)}{h_{ave.}\left(T_{wall} - T_f\right)} \quad (9)$$

The efficiency factor of rectangular and triangular fins for different conditions at angles of 0, 45, and 90 degrees is provided in Table. 5.

The average efficiency factor for rectangular and triangular fins in various angle positions is also provided in Fig. 15.

By analyzing the efficiency factor data provided in Table. 5 and comparing the averages at position angles of 0, 45, and 90 degrees, it was discovered that the rectangular fin is more efficient than the triangular fin. Furthermore, when examining Fig. 15, which illustrates the impact of angular position on average efficiency, it was determined that changes in the angle do not significantly affect the efficiency factor of either fin.

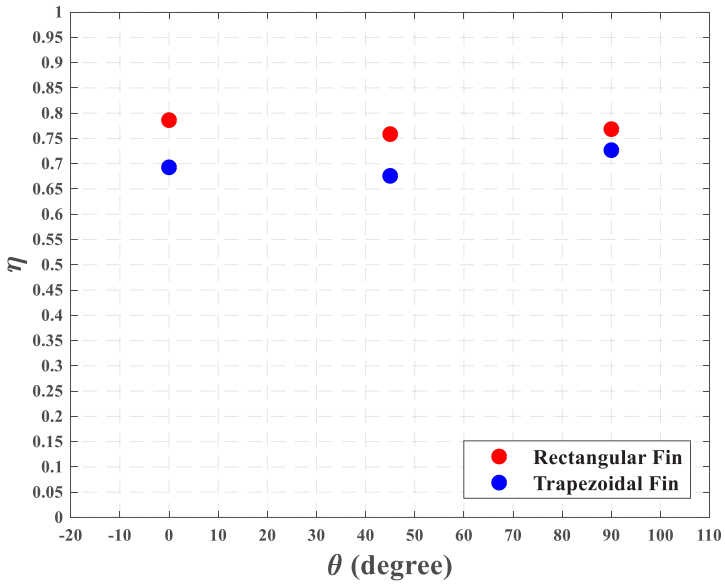

Fig. 15. The average efficiency for rectangular and triangular fins in different angles

5- 7- Pressure drop comparison

The pressure drop or resistance created by the fin against the passage of fluid flow is a key parameter in the design and fabrication of the cooling system that dissipates excess heat through an extended surface. In this case, the total pressure drop consists of three terms: friction, gravity, and momentum pressure drop. The frictional pressure drop is highly dependent on the flow velocity, the friction factor of the duct, and the quality of the fin surface by Eq. (10) [21].

$$dP_{fric.} \propto f \frac{L}{d} \rho V^2 \tag{10}$$

Also, the pressure drop caused by gravity in the fluid is provided in Eq. (11) [21].

$$dP_g \propto \rho g H \tag{11}$$

The pressure drop caused by the reduction of fluid flow momentum is determined from Eq. (12) [21].

$$dP_{mom.} \propto \rho V^2 \tag{12}$$

Since the cooling duct and fin surface have the same quality or friction factor for each experiment, the frictional pressure drop according to Eq. (10) will rely only on flow velocity. Additionally, because the forced convective mechanism is used, the pressure drop due to gravity will be negligible. Furthermore, the incompressibility properties of airflow cause the momentum pressure drop to only be influenced by flow velocity. Therefore, it is found that the total pressure drop for the fin cooling mechanism only relies on the cooling flow velocity.

Additionally, the cooling flow velocity is considered very low (M<<1). In this range, the flow velocity before the fin can be set by the downstream flow velocity. So, without the fin, the flow velocity will reach its maximum amount, and the anemometer will show the biggest value. If the fin creates a maximum pressure drop or is so big that it blocks the channel path, the upstream flow velocity before approaching the fin will start to reduce. In other words, if airflow velocity is assumed very low and the continuity is considered for airflow velocity, the effect of the velocity changes before and after the fin is directly on the flow velocity before the fin. The pressure drop of each fin geometry can be qualitatively compared to the upstream flow velocity. The flow speed is measured using an anemometer. According to Table. 6, the velocity of each fin for different angle positions was measured at the specific rotation speed of the fan blades.

According to Table. 6, the pressure drop or resistance created by the fin against the cooling flow passing through can be compared qualitatively. It was found that the pressure drop of the triangular fin was less than that of the rectangular fin, likely due to the sharp tip. Additionally, the pressure

Table 6. The maximum velocity of the cooling flow at a different angle

Fin Type	Fan Rotation Speed (rev/sec)	Angle (degree)	Maximum Air Velocity (m/sec)
	4000	90	1.8
Rectangular	4000	45	2.14
	4000	0	2.11
	4000	90	2
Triangular	4000	45	1.4
	4000	0	2.36

drop at an angle of 0 degrees had the lowest value compared to other positions. This could be attributed to the lowest resistance of the cross-section of the fin against the cooling flow at a position of 0 degrees.

5- 8- Uncertainty Analysis

Calculating uncertainty in measurement is one of the most important issues in experimental investigation. The uncertainty of an equation with several independent variables is measured by Eq. (13) [22]

$$H = H\left(X_1, X_2, ..., X_i\right) \Rightarrow$$

$$\delta H = \left\{ \sum_{i=1}^{N} \left(\frac{\delta H}{\delta X_i} \delta X_i \right)^2 \right\}^{0.5} \tag{13}$$

The term of $\frac{\delta H}{\delta X_i}$ is calculated mathematically and is related to the accuracy of the measuring equipment. This accuracy is provided in Table. 7 for the present study.

Therefore, the convective heat transfer coefficient which is a function of temperatures and heating thickness was calculated as Eq. (14).

$$\left.\begin{array}{l} h_{ave} = \dfrac{h_l + h_r + h_u + h_d}{4} \\ and \\ h_{l,r,u,d} = h\left(T_c, T_f, T_{l,r,u,d}, y\right) \end{array}\right\} \Rightarrow$$

$$h_{ave} = H\left(T_c, T_f, T_{l,r,u,d}, y\right) \tag{14}$$

Therefore, the uncertainty of the average HTC can be calculated using Eq. (15)

$$\%uncertanty = \frac{dh_{ave}}{h_{ave}}$$

$$dh_{ave} = [\left(\frac{\partial h_{ave}}{\partial h_l} dh_l \right)^2 + \left(\frac{\partial h_{ave}}{\partial h_r} dh_r \right)^2 + \left(\frac{\partial h_{ave}}{\partial h_u} dh_u \right)^2 + \left(\frac{\partial h_{ave}}{\partial h_d} dh_d \right)^2]^{0.5} \tag{15}$$

and

$$dh_{l,r,u,d} = [\left(\frac{\partial h_{l,r,u,d}}{\partial T_c} dT_c \right)^2 + \left(\frac{\partial h_{l,r,u,d}}{\partial T_{l,r,u,d}} dT_{l,r,u,d} \right)^2 + \left(\frac{\partial h_{l,r,u,d}}{\partial T_f} dT_f \right)^2 + \left(\frac{\partial h_{l,r,u,d}}{\partial y} dy \right)^2]^{0.5}$$

According to Eq. (14-15), the uncertainty of the heat transfer coefficient for all conditions is calculated and presented in Table. 8.

6- Conclusion

In this study, the effect of the main parameter of heat transfer of the fins is experimentally investigated. Factors such as practical geometry, wall heat flux, coolant velocity, and the impact angle by the fin are considered. The results are as follows:

I. The wide tip of the rectangular fin creates stagnation or vorticity in the cooling flow on the fin surface, leading to successive increases or decreases in the Heat Transfer Coefficient (HTC).

II. The sharp tip of the triangular fin can remove many vorticities or noise patterns in the cooling flow, resulting

Table 7. The accuracy of experimental parameters

parameter	equipment	uncertainty
Surface temperature	PT-100 sensor	±0.1 °C
distance	Digital caliper	±0.05 mm
electrical voltage	Multi-tester	±0.1 v
electrical resistance	Multi-tester	±0.1 Ω
Contact angle	Protractor	±1 degree
flow velocity	anemometer	±0.1 m/s
flow temperature	anemometer	±0.1 °C

Table 8. The average uncertainty value of HTC for different conditions in contact angles of 0, 45, and 90 degrees

Fin geometry	Flow contact angle (degree)	% mean HTC uncertainty
rectangular	90	0.68
rectangular	45	0.67
rectangular	0	0.68
triangular	90	0.70
triangular	45	0.78
triangular	0	0.70

in a more regular behavior of the HTC curve.

III. By removing vorticity, stagnation, or any noise related to the cooling flow, the triangular fin provides a higher convective heat transfer coefficient than the rectangular fin.

IV. A dimensionless number, Nu*, was introduced to consider the conductive mechanism alongside the convective heat transfer mechanism. Nu* of the rectangular fin was higher than the triangular fin. This means that the conductive heat transfer of a rectangular fin can compensate for the lower convective heat transfer caused by its larger volume or weight.

V. The results of temperature distribution along the rectangular and triangular fins show that due to its lower volume or weight, the triangular fin is more energy-efficient than the rectangular fin. Additionally, the temperature distribution curve of the rectangular fin has a lower local slope than the triangular fin, resulting in a greater efficiency for the rectangular fin.

VI. To consider the effect of wall or cooling flow temperature on the temperature distribution along the fin, a dimensionless number, θ*, was introduced. Comparing this number between the fins revealed that the temperature distribution along the rectangular fin was closer to the unique line (or wall temperature) than the triangular fin. Therefore, the rectangular fin is more efficient compared to the triangular fin.

VII. The efficiency factor was calculated for rectangular and triangular geometries at different angles and other conditions. The effect of angular position on the efficiency factor showed that angle variation does not significantly affect the efficiency of rectangular and triangular fins.

VIII. The study showed that the total pressure drop to fluid flow velocity is more dependent. The pressure drop at different angles was qualitatively compared for each fin based on the flow velocity data at specific fan rotation speeds. The results showed that: First: The pressure drop in a triangular fin is less than in a rectangular fin because the tip of a triangular fin is sharp and the tip of a rectangular wing is wide. Second: because in the position of zero degree angle, the resistance of the fin decreases against the cooling flow, the pressure drop is less than in other positions.

Nomenclature

h	Convective Heat Transfer Coefficient (W/m^2K)
HTC	Convective Heat Transfer Coefficient (W/m^2K)
K	Conductive Heat Transfer Coefficient (W/mK)
V	Velocity (m/s)
T	Temperature (°C)
Q''	Heat Flux (W/m^2)
L	Length (m)
D	Hydraulic Diameter (m)
Nu	Nusselt Number of fluid flow
$Nu*$	Dimensionless Heat Transfer of Fin
g	gravity acceleration (m/s^2)
H	height (m)
y	Heating thickness (half of fin thickness)

Subscripts

s	surface
$ave.$	average
$surf.$	Surface
l	left side
r	right side
u	upper side
d	downside
c	central
f	fluid
$fric.$	friction
g	gravity
$mom.$	Momentum
w	the root of the fin

Greek Symbols

η	efficiency factor
θ	dimensionless temperature
ρ	density (Kg/m^3)

References

[1] S.S. Chandrakant, S. Sunilkumar, N. Gokhale, Numerical and experimental analysis of heat transfer through various types of fin profiles by forced convection, International Journal of Engineering Research & Technology (IJERT), 2(7) (2013) 2278-0181.

[2] B. Freegah, A.A. Hussain, A.H. Falih, H. Towsyfyan, CFD analysis of heat transfer enhancement in plate-fin heat sinks with fillet profile: Investigation of new designs, Thermal Science and Engineering Progress, 17 (2020) 100458.

[3] S. Zaidshah, V. Yadav, Heat transfer from different types of fins with notches with varying materials to enhance rate of heat transfer a Review, international journal of applied engineering research, 14(9) (2019) 174-179.

[4] A. Tariq, K. Altaf, S.W. Ahmad, G. Hussain, T. Ratlamwala, Comparative numerical and experimental analysis of thermal and hydraulic performance of improved plate fin heat sinks, Applied Thermal Engineering, 182 (2021) 115949.

[5] P. Prasad, L. Prasad, Cfd analysis on louvered fin, Int Res J Eng Technol, 4(1) (2017) 1458-1462.

[6] A. Hashem-ol-Hosseini, M.A. Ghazani, M.D. Emami, Experimental study and numerical simulation of thermal hydraulic characteristics of a finned oval tube at different fin configurations, International Journal of Thermal Sciences, 151 (2020) 106255.

[7] A. Shadlaghani, M. Tavakoli, M. Farzaneh, M. Salimpour, Optimization of triangular fins with/without longitudinal perforate for thermal performance enhancement, Journal of Mechanical Science and Technology, 30 (2016) 1903-1910.

[8] B. Jalili, N. Aghaee, P. Jalili, D.D. Ganji, Novel usage of the curved rectangular fin on the heat transfer of a double-pipe heat exchanger with a nanofluid, Case Studies in Thermal Engineering, 35 (2022) 102086.

[9] M.A. Ali, S. Kherde, Design Modification and Analysis of Two-Wheeler Cooling Fins-A Review, International Journal of Advances in Engineering & Technology, 7(3) (2014) 998-1002.

[10] I. Satyanarayana, G. Pranay, Design and analysis of rectangular and triangular fins using CFD, International Journal of Scientific Engineering and Technology Research, 5(31) (2016) 6554-6564.

[11] R. Vijayakumar, T. Nithyanandam, A. Janarthanan, N. Jeevanantham, B. Santhosh, Analysis of Rectangular Fins Using CFD, Annals of the Romanian Society for Cell Biology, (2021) 1892-1898.

[12] P.K. Singh, V.K. Sharma, A. Islam, Numerical analysis on thermal properties of aluminium alloy for transforming heat based applications, Materials Today: Proceedings, 45 (2021) 3596-3600.

[13] S. Durgam, A. Kale, N. Kene, A. Khedkar, S. Palve, N.M. Gawai, Thermal analysis of fin materials for engine cylinder heat transfer enhancement, in: IOP Conference Series: Materials Science and Engineering, IOP Publishing, 2021, pp. 012071.

[14] S. Mirapalli, P. Kishore, Heat transfer analysis on a triangular fin, Int J Eng Trends Technol, 19(5) (2015).

[15] M. Torabi, A. Aziz, K. Zhang, A comparative study of longitudinal fins of rectangular, trapezoidal and concave parabolic profiles with multiple nonlinearities, Energy, 51 (2013) 243-256.

[16] R. Karvinen, T. Karvinen, Optimum geometry of plate fins, Journal of heat transfer, 134(8) (2012).

[17] T.L. Bergman, A.S. Lavine, F.P. Incropera, D.P. DeWitt, Introduction to heat transfer, John Wiley & Sons, 2011.

[18] C.-H. Huang, P.-W. Tung, Numerical and experimental studies on an optimum Fin design problem to determine the deformed wavy-shaped heat sinks, International Journal of Thermal Sciences, 151 (2020) 106282.

[19] E. Buckingham, On physically similar systems; illustrations of the use of dimensional equations, Physical review, 4(4) (1914) 345.

[20] M. Pourjafargholi, A. R. Gholami, and M. R. Karimi, "Investigating fin heat transfer in rectangular, triangular and parabolic geometries in singular and groups under laminar and turbulent cooling airflow," Journal of Aerospace Defense, vol. 2, no. 2, pp. 55-83, (2023).

[21] J.G. Collier, J.R. Thome, Convective boiling and condensation, Clarendon Press, 1994.

[22] R.J. Moffat, Describing the uncertainties in experimental results, Experimental thermal and fluid science, 1(1) (1988) 3-17.

.Appendix A

A-1. Summary of Pi-Buckingham theorem

According to the Pi-Buckingham theorem, to reduce computational cost, the number of effective variables in a physical phenomenon is studied in groups. These groups are formed by the product of parameters that neutralize each other's dimensions and provide dimensionless groups for simulation. If the number of effective parameters in a physical phenomenon is n and the number of fundamental quantities (including length *L*, mass *M*, temperature *K*, and time *T*) is also m, then the number of similarity variables can be calculated by Eq. (a).

$$r = n - m \tag{a}$$

Finally, Eq. (b) expresses the relationship between these groups. According to this equation, the group containing the main variable being considered is positioned on the left side, while the other groups are placed on the right side.

$$\Pi_1 = F\left(\Pi_2, \Pi_3, \Pi_4, ..., \Pi_r\right) \tag{b}$$

Furthermore, based on experimental data, the values of the dimensionless groups at the points of interest are obtained, and the dependency function of the main group on the other groups is calculated. According to Eq. (c), to determine the main parameter of interest in an industrial phenomenon, the corresponding group must be equal under both industrial and experimental conditions. In other words, there must be a similarity in group Π_1 between the actual and experimental phenomena. This equality can only be achieved if the other dimensionless groups are also the same in both industrial and experimental conditions.

$$\Pi_1 = F\left(\Pi_2, \Pi_3, \Pi_4, ..., \Pi_r\right)$$

$$If \quad \Pi_{2,\exp} = \Pi_{2,real} \;, \Pi_{3,\exp} = \Pi_{3,real} \;, \Pi_{4,\exp} = \Pi_{4,real} \tag{c}$$

$$Thus \Rightarrow \quad \Pi_{1,real} = \Pi_{1,\exp} \Rightarrow P_{real} \text{ will be determined}$$

A-2. Developing the dimensionless groups

Table. A displays the effective parameters in fin heat transfer, along with their corresponding quantities. It is also necessary to choose specific parameters, such as the main quantities, from among the parameters being considered.

Table A: The effective parameter on HTC with related quantity

	Parameter	Variable	Symbol	Quantity
1	Applied heat flux	Heat flux	Q''	MT^{-3}
2	Coolant flow velocity	Velocity	V	LT^{-1}
3	Fin root area	Area	A_g	L^2
4	Fin length	Length	L	L
5	Surface temperature	Temperature	T_r	K
6	Fluid temperature	Temperature	T_f	K
7	Average heat transfer coefficient	Heat transfer coefficient	h	$MT^{-3}K^{-1}$
8	Fluid density	Density	ρ_f	ML^{-3}
9	Fluid viscosity	Viscosity	μ_f	$ML^{-1}T^{-1}$
10	Fluid thermal conductivity	Thermal conductivity	K_f	$MT^{-3}K^{-1}L$
11	Fin density	Density	ρ_s	ML^{-3}
12	Fin thermal conductivity	Thermal conductivity	K_s	$MT^{-3}K^{-1}L$
13	Fluid-specific heat at constant pressure	Specific heat	Cp_f	$L^2T^{-2}K^{-1}$
14	Fin specific heat	Specific heat	Cp_s	$L^2T^{-2}K^{-1}$

The selected parameters in the present study are V, L, ρf, and Ks. According to equations (a) and (b), the number of dimensionless groups can be determined using Eq. (d).

$$r = 14 - 4 = 10$$
$$\Pi_1 = \Phi\left(\Pi_2, \Pi_3, \Pi_4, ..., \Pi_9\right) \quad \textbf{(d)}$$

In order to form any dimensionless group, an arbitrary parameter must be multiplied by all selected parameters with parametric exponents, and then the sum of the exponents of each quantity should be set

equal to zero to eliminate dimensions. For example, group Π_1 will be calculated according to Eq. (e). Since the temperature of the hot surface in contact with the blade can be considered the main parameter in the design of the cooling blades, this parameter will be included in the Π_1 group.

$$\Pi_1 = T_r \rho_f{}^a V_f{}^b L^c K_s{}^d$$

$$\Rightarrow \left[\Pi_1\right] = K\left(ML^{-3}\right)^a \left(LT^{-1}\right)^b \left(L\right)^c \left(MLT^{-3}K^{-1}\right)^d \quad \textbf{(e)}$$

$$\Rightarrow \left[\Pi_1\right] = K^{(1-d)} M^{(a+b)} L^{(-3a+b+c+d)} T^{(-b-3a)} = K^0 M^0 L^0 T^0$$

$$\Rightarrow a = 1\ ,\ b = -3\ ,\ c = -1,\ d = 1$$

In conclusion, the main dimensionless group containing the surface temperature can be obtained from Eq. (f).

$$\Pi_1 = \frac{T_r K_s}{\rho_f V^3 L} \quad \textbf{(f)}$$

Similarly, all dimensionless groups can be obtained as shown in Table. B.

Table B: The dimensionless groups of present study base on Pi-Buckingham groups.

Dimensionless group	relation	Dimensionless group	relation
Π_1	$\frac{T_r K_s}{\rho_f V^3 L}$	Π_6	$\frac{\mu_f}{\rho_f VL}$
Π_2	$\frac{Q''}{\rho_f V^3}$	Π_7	$\frac{K_f}{K_s}$
Π_3	$\frac{A_c}{L^2}$	Π_8	$\frac{\rho_s}{\rho_f}$
Π_4	$\frac{T_f K_s}{\rho_f V^3 L}$	Π_9	$\frac{Cp_s \rho_f VL}{K_s}$
Π_5	$\frac{hL}{K_s}$	Π_{10}	$\frac{Cp_f \rho_f VL}{K_s}$

Finally, based on Eq. (c), the final correlation between dimensionless groups is calculated as Eq. (g).

$$\frac{T_r K_s}{\rho_f V^3 L} = \Phi\left(\frac{Q''}{\rho_f V^3}, \frac{A_c}{L^2}, \frac{T_f K_s}{\rho_f V^3 L}, \frac{hL}{K_s}, \frac{\mu_f}{\rho_f VL}, \frac{K_f}{K_s}, \frac{\rho_s}{\rho_f}, \frac{Cp_s \rho_f VL}{K_s}, \frac{Cp_f \rho_f VL}{K_s}\right) \quad \textbf{(g)}$$

Since the Huang-Tung study and the present study share the same parameters, such as fluid type, flow velocity, and aluminum fins, the $\Pi_{1\text{-}3}$ group was selected as the primary and most effective group for comparison.

HOW TO CITE THIS ARTICLE
Mohammad Pourjafargholi, Alireza Gholami, Mohammadreza Karimi, Experimental investigation of fin heat transfer characteristics in different condition, AUT J. Mech Eng., 8(2) (2024) 151-180.

DOI: 10.22060/ajme.2024.23065.6096